

American Journal of Science

MARCH 1996

CYCLING OF IRON AND MANGANESE IN SURFACE SEDIMENTS: A GENERAL THEORY FOR THE COUPLED TRANSPORT AND REACTION OF CARBON, OXYGEN, NITROGEN, SULFUR, IRON, AND MANGANESE

PHILIPPE VAN CAPPELLEN and YIFENG WANG

School of Earth and Atmospheric Sciences,
Georgia Institute of Technology,
Atlanta, Georgia 30332

ABSTRACT. This paper presents a multicomponent early diagenetic model which explicitly accounts for the coupling of the redox cycles of Fe and Mn to those of oxygen, carbon, sulfur, and nitrogen. Rate expressions are used to represent the oxidation of organic carbon, the oxidation of secondary reduced species formed as byproducts of organic matter oxidation, and the precipitation and dissolution of sulfide and carbonate minerals. The net rate of organic carbon oxidation is broken down into the contributions of aerobic respiration, denitrification, dissimilatory Mn(IV) reduction, dissimilatory Fe(III) reduction, sulfate reduction, and methanogenesis. The computational algorithm is based on a modified Monod kinetics formulation for the organic matter degradation pathways. The non-specific adsorption of ammonia, the surface complexation of Fe^{2+} and Mn^{2+} cations, and the homogeneous interconversions within the dissolved carbonate-sulfide system are treated as equilibrium reactions. The transport processes included are sediment advection, pore water diffusion, and particle mixing and irrigation by benthic macrofauna. Chemical component concentrations and pore water alkalinity are described by a set of continuity equations characterized by nonlinear reaction rate terms. The equations are solved by finite-difference. The distribution of pore water pH is derived from the calculated profiles of total dissolved inorganic carbon, total dissolved sulfide, and alkalinity. Particulate deposition fluxes and bottom water composition are imposed as upper boundary conditions.

The model is applied to an extensive set of data collected in a marine sediment from the Skagerrak (Denmark). Theoretical depth profiles reproduce the measured pore water concentrations of O_2 , NO_3^- , NH_4^+ , Mn^{2+} , and Fe^{2+} plus the solid sediment concentrations of Fe(III), Mn(IV), sulfide-bound Fe(II), and non-sulfide Fe(II). The model also correctly simulates the depth distribution of measured sulfate reduction rates. According to the computations, approximately two thirds of the total rate of iron reduction in the sediment are utilized directly by bacteria to oxidize organic carbon (dissimilatory Fe reduction). Manganese reduction, on the other hand, is mostly due to chemical reaction with dissolved Fe^{2+} . Despite the relatively high rates of iron and manganese reduction, only very small amounts of the Fe(II) and

Mn(II) produced during early diagenesis are permanently buried in the deeper sediment. Most of the dissolved and solid-bound Fe(II) and Mn(II) cations reoxidize in the surface sediment or escape to the water column. The main oxidation pathways in the sediment are heterogeneous oxygenation of surface complexed Fe^{2+} and Mn^{2+} cations. The model also predicts that intense redox cycling of Fe and Mn should cause the appearance of a pH minimum at the base of the aerobic surface layer.

INTRODUCTION

The transformations of iron and manganese are key processes in the biogeochemistry of marine and freshwater sediments. The oxides and oxyhydroxides (henceforth referred to as (hydr)oxides) of iron and manganese reductively dissolve upon burial or mixing below the aerobic surface layer of sediments underlying oxygenated bottom waters. Pore water Fe(II) and Mn(II) produced within the anaerobic zone may adsorb onto sediment particles, (co)precipitate as authigenic sulfide, carbonate, and phosphate mineral phases, or be transported back toward the water-sediment interface via pore water diffusion and irrigation. A fraction of the particle-bound Fe(II) and Mn(II) may also be returned to the oxidized surface layer of the sediment through particle mixing induced by benthic macrofaunal activity. Upon encountering more oxidizing conditions, the reduced Fe(II) and Mn(II) reoxidize and precipitate as (hydr)oxides.

The coupling of redox transformations and transport processes gives rise to the cycling of iron and manganese between the aerobic and anaerobic portions of surface sediments. An iron or manganese cation deposited at the water-sediment interface may cycle many times through its oxidized and reduced states before being buried permanently below the zone of active early diagenesis. Consequently, the electron fluxes associated with the iron and manganese cycles in a sediment may greatly exceed the electron acceptor capacities supplied by deposition of Fe and Mn (hydr)oxides from the oxygenated water column. The redox cycling of iron and manganese also plays an important role in the early diagenetic behavior of numerous other elements, including phosphorus and trace metals (Froelich and others, 1979; Krom and Berner, 1981; Shimmiel and Pedersen, 1990).

The general outline of the early diagenetic redox cycles of iron and manganese given above has been known for many years (Lynn and Bonatti, 1965). Recent work, however, has revealed that the cycles are much more complex than previously envisioned (Canfield, Thamdrup, and Hansen, 1993; Aller, 1994). In particular, it is now clearly established that the reduction and oxidation of iron and manganese in natural aquatic systems may proceed via a variety of pathways. Microorganisms can couple the reduction of iron and manganese (hydr)oxides directly to organic matter oxidation (Lovley, 1987, 1991; Nealson and Myers, 1992; Burdige, 1993; DiChristina and DeLong, 1993). Dissimilatory iron and manganese reduction, however, compete with the chemical reduction of

the (hydr)oxides by a variety of inorganic and organic reductants (Berner, 1970; Postma, 1985; Stone, 1987; Wehrli, Sulzberger, and Stumm, 1989; Luther and others, 1992; Sunda and Kieber, 1994). Manganese (hydr)oxides, for instance, may be reduced by pore water Fe^{2+} (Postma, 1985; Myers and Nealson, 1988; Burdige, Dhakar, and Nealson, 1992), while both iron and manganese (hydr)oxides are reductively dissolved through reaction with sulfide (Pyzik and Sommer, 1981; Burdige and Nealson, 1986; Canfield and Berner, 1987; Yao and Millero, 1993). Similarly, a variety of microbial and abiotic oxidation pathways of reduced iron and manganese species have been documented in natural aquatic environments (Sung and Morgan, 1980; Davison and Seed, 1983; Emerson and others, 1982; Sunda and Huntsman, 1990; Luther and others, 1992; Stumm and Sulzberger, 1992).

Previously published models of early diagenesis have not, to our knowledge, explored the possibility of multiple pathways of oxidation and reduction of Fe and Mn in sediments. Existing models of manganese or iron cycling capture the oxidation or reduction of the metal in a single rate expression. Furthermore, it has been commonly assumed that the rate laws describing oxidation and reduction depend only on the concentrations of the reduced and oxidized forms of the metal itself or obey *a priori* imposed depth distributions (Michard, 1971; Robbins and Callender, 1975; Burdige and Gieskes, 1983; Gratton and others, 1990; Wersin and others, 1991). With these assumptions, the conservation equations of the metal species can be solved independently from the distributions of other chemical elements. However, it also means that the models are limited in their ability to simulate the coupled, multicomponent chemical dynamics of early diagenetic systems. In this respect, the models of Aller (1990) and Rabouille and Gaillard (1991) represent a step forward, because they link the redox transformations of manganese to those of organic carbon and oxygen.

In this paper, we extend the earlier theoretical work by developing a transport-reaction model that explicitly accounts for the coupling of the redox cycles of iron, manganese, oxygen, carbon, sulfur, and nitrogen. The model solves simultaneously the continuity equations representing mass conservation of all the independent reactive chemical species involved in controlling the spatial and temporal distributions of iron and manganese (table 1). Each individual reaction pathway that produces or consumes reactive species is included in the appropriate conservation equations, either as a rate expression or, for very fast reactions, as an equilibrium constraint. The equations of the independent species must be solved together, because they are coupled through the reaction rate terms. The result is an early diagenetic model in which the downward succession of reaction zones comes about naturally as the result of the production, consumption, and transport of all reactive species. There is no longer a need to assign beforehand the depth distribution of chemical conditions in the sediment in order to predict the distributions of iron and manganese.

TABLE 1

Dissolved, interfacial and solid species included in the model. $\equiv S - H^0$ corresponds to a hydrated surface site. The chemical formula used to represent sedimentary organic matter assumes an average oxidation state of zero for organic carbon

Dissolved species	O_2	
	NO_3^-	
	Mn^{2+}	
	Fe^{2+}	
	SO_4^{2-}	
	NH_4^+	
	CH_4	
	$CO_2(aq), HCO_3^-, CO_3^{2-}$	
	H_2S, HS^-	
	H^+	
	Interfacial species	$\equiv S - H^0$
		$\equiv S - Mn^+$
		$\equiv S - Fe^+$
Solid species	$NH_4^+(ads)$	
	$(CH_2O)_x(NH_3)_y(H_3PO_4)_z$	
	MnO_2	
	$Fe(OH)_3$	
	$Ca_{1-x}Mn_xCO_3$	
	$Ca_{1-x}Fe_xCO_3$	
	FeS	

REACTIVE SPECIES

The first step in constructing the early diagenetic model for iron and manganese is the choice of the reactive chemical species (table 1). The species include the various dissolved, interfacial, and solid forms of the metals themselves, as well as other pore water and particulate constituents that affect the rates and loci of production and consumption of Fe and Mn species in the sediment.

In contrast to earlier models, adsorbed iron and manganese cations are included as separate species in our model. Interfacial Fe(II) and Mn(II) are critical reaction intermediates in the oxidative transformations of the metals (Morgan, Sung, and Stone, 1985). Furthermore, adsorbed Fe(II) and Mn(II) may represent significant fractions of solid-bound metals in surface sediments (Murray, Balistrieri, and Paul, 1984; Canfield, Thamdrup, and Hansen, 1993; this work).

The solid phases $Fe(OH)_3$ and MnO_2 are used as idealized representations of the reactive, bioavailable fractions of oxidized iron and manganese (hydr)oxides. Iron monosulfide, FeS , is the initial Fe(II) sulfide precipitate forming in anoxic sediments as the result of sulfate reduction (Bernier, 1984). The kinetically-favored FeS is used in the model because it controls pore water iron concentrations in sulfide-producing sediments, rather than the thermodynamically more stable pyrite (Boudreau

and Canfield, 1988). Carbonate alkalinity production during anaerobic respiration may lead to the precipitation of carbonate minerals. In freshwater sediments, relatively pure FeCO_3 and MnCO_3 may form (Emerson, 1976; Wersin and others, 1991). In marine depositional environments, however, the formation of solid solutions with CaCO_3 is more likely, especially for Mn(II) (Pedersen and Price, 1982; Mucci, 1988; Jakobsen and Postma, 1989; Gaillard, Pauwels, and Michard, 1989).

With the exception of particulate organic matter and adsorbed ammonia, the remaining species in table 1 are solutes. They correspond to the principal redox and acid-base species found in natural pore waters. Typically, the vertical profiles of these species are used to define the distribution of geochemical zones in sediments (Froelich and others, 1979).

The set of reactive species in table 1 offers a simplified description of the composition of sediments and pore waters. Nonetheless, it does provide the model with the essential actors needed to simulate at a fairly realistic level the chemical complexity of early diagenetic systems. Furthermore, it is important to note that the modeling approach adopted here is completely general and that, in theory, there is no limit to the number of species and reactions that can be included.

REACTIONS

Most biogeochemical transformations affecting iron and manganese in surface sediments are driven, directly or indirectly, by the decomposition of organic matter. The supply of organic detritus from the water column is the ultimate source of energy for the microbial and macrofaunal populations that inhabit a surface sediment. (Note: for sediments situated within the photic zone, organic matter supply may also originate from benthic primary production.) This external supply of metabolic energy maintains the overall state of thermodynamic disequilibrium of the surface sediment which is expressed, among other things, by the persistence of vertical gradients in chemical and biological properties.

The decomposition of organic matter is the result of many enzymatic reactions involving a variety of organisms and a variety of intermediate compounds. However, the net effect of organic matter decomposition on pore water and solid sediment composition can be represented by overall reactions (Van Cappellen, Gaillard, and Rabouille, 1993). The idealized net decomposition reactions included in the model are listed in table 2. They include oxic respiration (eq 1), denitrification (eq 2), manganese (hydr)oxide reduction (eq 3), iron (hydr)oxide reduction (eq 4), sulfate reduction (eq 5), and methanogenesis (eq 6). The reactions are listed roughly in the sequence in which they occur with increasing depth in a sediment. The sequence reflects the order of decreasing energy yield of the oxidation reactions (Berner, 1980).

Reactions (1) to (6) are termed the primary redox reactions with organic carbon acting as the reductant. The oxidation of organic matter

TABLE 2

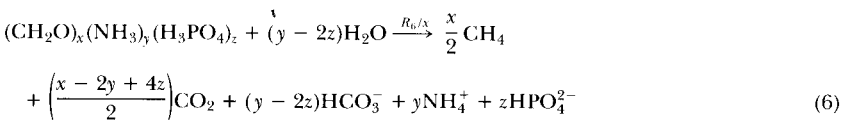
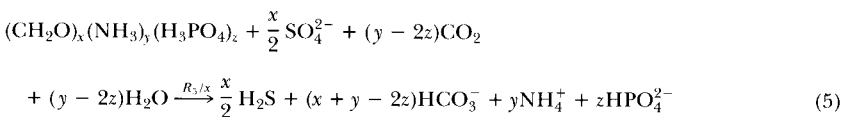
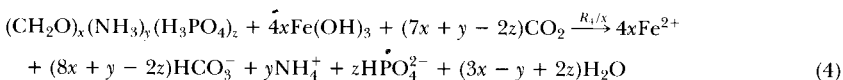
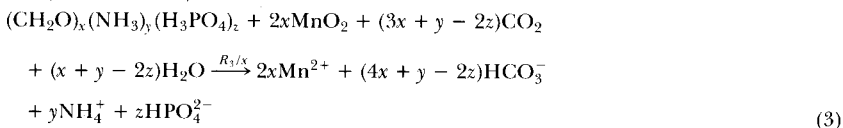
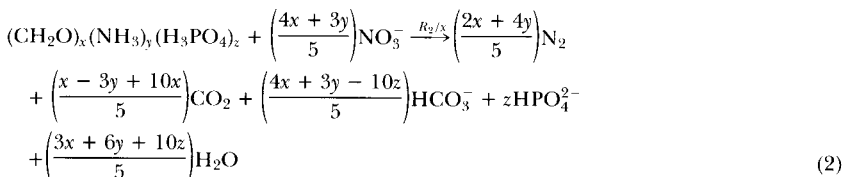
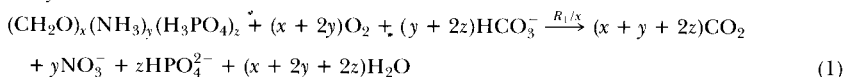
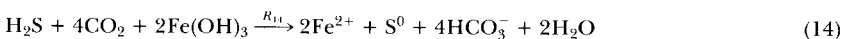
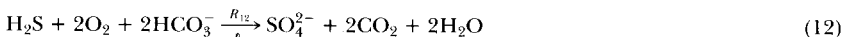
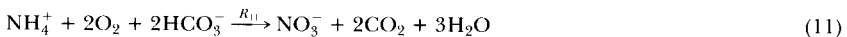
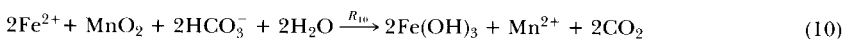
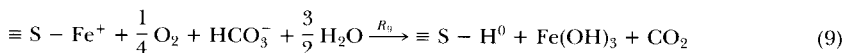
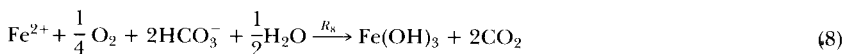
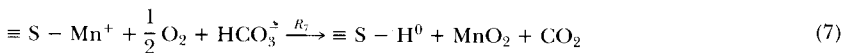
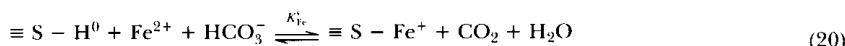
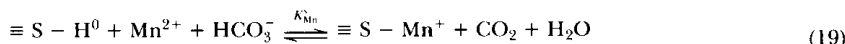
*Biogeochemical reactions included in the model**Primary redox reactions:**Secondary redox reactions:*

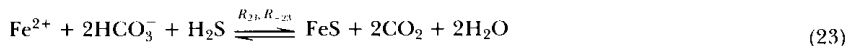
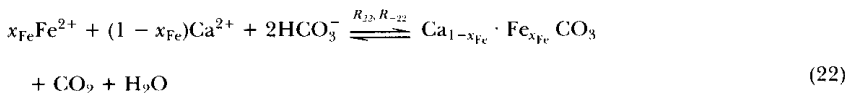
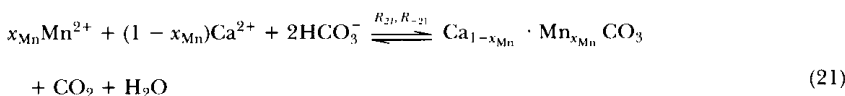
TABLE 2
(continued)



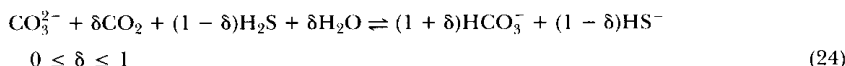
Adsorption reactions:



Precipitation and dissolution reactions (non-redox):



Alkalinity conservation:



produces the reduced pore water species Mn^{2+} , Fe^{2+} , NH_4^+ , H_2S , and CH_4 , which may participate in secondary redox reactions, adsorb onto sediment particles, or (co)precipitate from solution (eqs 7-23). Many of the secondary redox reactions listed in table 2 may be catalyzed by microorganisms (Chapelle, 1993).

The model considers only the heterogeneous oxygenation of manganese(II) (eq 7) because of the exceedingly slow kinetics of the homogeneous reaction of Mn^{2+} with oxygen (Diem and Stumm, 1984). For iron, however, both homogeneous (eq 8) and heterogeneous (eq 9) oxygenation may proceed at measurable rates in natural aquatic environments (Davison and Seed, 1983; Wehrli, 1990). In addition, Fe^{2+} may be oxidized through reaction with manganese (hydr)oxides (eq 10) (Postma, 1985; De Vitre and others, 1988; Myers and Neelson, 1988; Burdige, Dhakar, and Neelson, 1992).

Net nitrification is represented by reaction (11) (Billen, 1982), pore water sulfide oxidation by reactions (12), (13), and (14) (Millero and others, 1987; Yao and Millero, 1993; Canfield, Raiswell, and Bottrell, 1992), and methane oxidation by reactions (16) and (17) (Berner, 1980; Devol and others, 1984; Iversen and Jørgensen, 1985). Note that pore water sulfide directly competes with organic carbon as reductant for the dissolution of iron and manganese (hydr)oxides in reactions (13) and (14). Reaction (15) accounts for the oxidative dissolution of authigenic iron sulfide mineral brought up into the aerobic zone via sediment mixing.

Ammonia adsorption (eq 18) is treated as a reversible, non-specific cation exchange reaction (Grim, 1968). The adsorption reactions of the metal cations Fe^{2+} and Mn^{2+} (eqs 19 and 20) are written as complexation reactions with hydrated surface sites (Davis and Kent, 1990; Dzombak and Morel, 1990). Adsorption sites for Fe^{2+} and Mn^{2+} in natural sediments are predominantly located on the surfaces of Fe/Mn (hydr)oxides and organic or biological particulates (Balistrieri, Brewer, and Murray, 1981; Lion, Altmann, and Leckie, 1982; Murray, Balistrieri, and Paul, 1984; Johnson, 1986; Sigg, 1987; Canfield, Thamdrup, and Hansen, 1993).

The profiles of dissolved Fe^{2+} and Mn^{2+} are often found to decrease with depth in the anaerobic portions of sediments. It is usually assumed that this reflects the precipitation of authigenic carbonate and sulfide mineral phases (eqs 21, 22, and 23). The model allows for both the precipitation and dissolution of the authigenic minerals. The coupling of the non-oxidative dissolution of iron sulfide (eq 23) to dissolved sulfide oxidation by manganese or iron (hydr)oxides (eqs 13 and 14) provides pathways for the oxidation of FeS in the absence of molecular oxygen. Aller and Rude (1988) have demonstrated experimentally that Mn oxides and possibly also Fe (hydr)oxides can oxidize solid phase sulfide in anoxic marine sediments (see also Canfield, Thamdrup, and Hansen, 1993).

The principal weak acids in natural pore waters are carbonic acid and, when sulfate reduction is important, hydrogen sulfide. In the model, we assume that the pore water pH is determined by the extent of dissociation of these two acids. Buffering is included in the model by writing reactions (1) to (23) in such a manner that any production or consumption of protons is balanced by rapid bicarbonate-carbonic acid interconversion. Consequently, the reaction stoichiometries describe the net production of pore water alkalinity by reactions (1) to (23). Local pH balance and alkalinity conservation is modeled by assuming internal equilibrium among the dissolved carbonate and sulfide species (reaction 24).

RATE LAWS AND EQUILIBRIUM CONDITIONS

Primary redox reactions.—Most kinetic descriptions of organic matter degradation used in early diagenetic models derive from the simple

first-order kinetic model (*G*-model) originally introduced by Berner (1964):

$$R_C = - \frac{d[\text{CH}_2\text{O}]}{dt} = k_C [\text{CH}_2\text{O}]_m \quad (25)$$

where R_C corresponds to the net rate of organic carbon oxidation, k_C is a first-order rate coefficient, $[\text{CH}_2\text{O}]$ is the concentration of organic carbon, and the subscript m refers to the metabolizable fraction of the organic carbon.

In the simplest possible approach, the rate coefficient k_C in eq (25) is assigned a single value, representative of the average reactivity of the sedimentary organic carbon over the depth range of interest (one-*G* model). More sophisticated *G*-type models which take into account the variability of organic matter reactivity with advancing degradation (for a recent review, see, Van Cappellen, Gaillard, and Rabouille, 1993) have been presented.

Several options for the total rate of organic carbon oxidation are available in the computer code we have developed. In one option, the user provides values for the deposition flux and rate coefficient of metabolizable organic carbon. The program then calculates the distributions of the carbon oxidation rate and the concentration of metabolizable organic carbon, using eq (25). In another option, the depth distribution of the total rate of organic carbon oxidation is imposed *a priori*. It is the latter option that is used in the simulations presented below. All options share one important feature: the total rate of organic carbon degradation is determined independently from the concentrations of species other than organic carbon. This is a characteristic inherent of the *G*-models for organic matter degradation (eq 25).

In the present model, the total rate of organic carbon oxidation is broken down into the contributions of the individual metabolic pathways represented by reactions (1) to (6). To this end, the model calculates the fractions f_i defined by

$$f_i = \frac{R_i}{R_C} \quad i = 1, \dots, 6 \quad (26)$$

where R_i is the rate of carbon oxidation by the i -th pathway. Obviously, the rates R_i satisfy the following condition:

$$R_C = \sum_{i=1}^6 R_i \quad (27)$$

To calculate fraction f_i , the model first determines whether the corresponding pathway is repressed by more energetic pathways. If not, the model checks whether the rate of the i -th pathway is limited or not by the availability of the external electron acceptor (note: this applies only to

the respiratory pathways, $i = 1$ to 5). The decision algorithm is based on a modified Monod formulation (Boudreau and Westrich, 1984; Gaillard and Rabouille, 1992) and assumes that for each of the five respiratory pathways there exists a critical or limiting concentration of the external oxidant. When the concentration of the oxidant exceeds the limiting value, the rate of the metabolic pathway is assumed to be independent of the concentration of the oxidant. In addition, the oxidation of organic carbon by energetically less powerful electron acceptors is inhibited. When the external oxidant concentration decreases below the limiting value, the rate is calculated by:

$$R_i = R_{\max} \frac{[EA]}{[EA]_{\text{lim}}} \quad \text{for } [EA] < [EA]_{\text{lim}} \quad (28)$$

where $[EA]$ is the concentration of the external oxidant, $[EA]_{\text{lim}}$ is the limiting concentration, and R_{\max} is the rate of oxidation when the supply of oxidant is not limiting ($[EA] \geq [EA]_{\text{lim}}$).

The modified Monod kinetic formulation insures that with the exhaustion of the electron acceptor the corresponding organic carbon oxidation pathway comes to a halt. Furthermore, when $[EA] < [EA]_{\text{lim}}$, the benthic heterotrophs begin utilizing oxidants with a lower intrinsic free energy yield. Use of the linear formulation of eq (28) increases computational efficiency and yields metabolic rate distributions that, for all practical purposes, are identical to those calculated with the full Monod law.

According to the computational procedure, methanogenesis (eq 6) is inhibited until the pore water sulfate concentration drops below its limiting value. When this happens, the contribution of methanogens to the overall degradation of organic carbon is calculated from:

$$f_6 = 1 - \sum_{i=1}^5 f_i \quad (29)$$

In the model, the effects of oxidant limitation, metabolic inhibitors, and competition are all incorporated into the limiting oxidant concentrations, $[EA]_{\text{lim}}$. Kinetic formulations for the inhibition of metabolic pathways and mechanisms for the competition between microbial populations have been presented in the literature (for a review, see, Van Cappellen, Gaillard, and Rabouille, 1993). Nonetheless, the implementation of oxidant limitation, inhibition, and competition as separate processes in the model would require a substantial number of additional parameters, most of which are poorly constrained. The use of a single $[EA]_{\text{lim}}$ value per respiratory pathway offers the simplest way to deal with the complex physiological and ecological interactions that control the distribution of oxidant utilization in a sediment. It should be understood, however, that the $[EA]_{\text{lim}}$ values represent apparent limiting concentrations, which may

deviate from true oxidant limiting concentrations, as measured for example in controlled microcosm experiments.

The calculation scheme developed for representing organic carbon breakdown and dissimilatory oxidant utilization results in smooth transitions between redox zones in the sediment column. The values of the limiting concentrations, $[EA]_{\text{lim}}$, control the extent of vertical overlap between the successive organic matter degradation pathways. The calculations require values for the limiting concentrations of the successive external electron acceptors, O_2 , NO_3^- , Mn(IV), Fe(III), and SO_4^{2-} . Order-of-magnitude estimates of the apparent limiting concentrations of the dissolved oxidants in natural aquatic environments are available (Van Cappellen, Gaillard, and Rabouille, 1993; table 6). To our knowledge, no limiting concentrations have been reported for iron and manganese (hydr)oxide utilization. As shown later in this paper, modeling of the early diagenetic distributions of iron and manganese provides a way to constrain the limiting concentrations of Mn(IV) and Fe(III).

Secondary redox reactions.—In inorganic studies of redox reactions, rates are shown to correlate positively with the concentrations of both the oxidant and reductant participating in the reaction. As mentioned earlier, many of the secondary redox reactions in table 2 may in fact be microbially mediated. Although microbial involvement adds a new level of complexity, one may still expect the reaction kinetics to be limited by the availability of the terminal electron donor and the terminal electron acceptor. For example, Tebo and Emerson (1985) have shown that, at low reactant concentrations, the rate of microbial oxidation of manganese correlates positively with the concentrations of both Mn(II) and oxygen.

The available kinetic information on chemical and microbial redox processes imposes two fundamental requirements on the sediment rate model. First, the model should restrict the occurrence of a secondary redox reaction to that portion of the sediment where both the oxidant and the reductant have non-zero concentrations. Second, the rate laws should depend on the concentrations of the oxidant and the reductant. The most straightforward way to meet those requirements is to use bimolecular reaction rate laws for the secondary redox reactions (table 3, eqs 31-41).

For a number of abiotic redox reactions, experimental evidence directly supports the bimolecular rate laws used in the model. The rates of abiotic oxygenation of iron and manganese (eqs 7, 8, and 9), for example, have been shown to be proportional to the concentrations of oxygen and surface-bound or dissolved metal cations (Stumm and Lee, 1961; Morgan, Sung, and Stone, 1985; Wehrli, 1990; Stumm, 1992). Similarly, the inorganic oxidation kinetics of sulfide by oxygen and MnO_2 follow bimolecular rate laws (Millero and others, 1987; Yao and Millero, 1993). In those instances where detailed experimental information is unavailable, the bimolecular rate law represents the simplest, yet kinetically consistent, way to deal with the inorganic kinetics of redox reactions.

